Vol. 14(1), pp. 14-24, October-December, 2023
DOI: 10.5897/JSSEM2023.0926
Article Number: 962598C71577
ISSN: 2141-2391

http://www.academicjournals.org/JSSEM

Journal of Soil Science and Environmental Management

Full Length Research Paper

Response of rainfall variability on the evolution of the vegetative cycle in the Chari-Logone basin (Lake Chad basin)

Mahamat Nour A.[1]*, Vallet-Coulomb[2], Sylvestre F.[1,2] and Deschamps P.[2]

[1]Laboratoire Hydro-Géosciences and Réservoirs, University of N'Djamena, N'Djamena, Chad.
[2]Aix Marseille Univ, CNRS, IRD, INRAE, Coll France, CEREGE, Aix-en-Provence, France.

Received 3 September, 2023; Accepted, 21 November, 2023

The Chari-Logone Basin (CLB), encompassing 610,000 km^2 as the hydrologically active segment of the Lake Chad basin, is the focal point of this study aiming to characterize the evolution of vegetation cover in response to rainfall. The primary focus relies on spatialized precipitation and NDVI data. Analysis of these spatial rainfall data reveals trends that predominantly align with a south-north gradient typical of the Sudano-Sahelian region, with the highest values observed in the southwestern part of the basin, coinciding with the direction of the monsoon flow into the area. The NDVI results depict spatial and seasonal changes, mirroring the seasonal variation in climate, particularly rainfall. In the Chari-Logone basin, the vegetation undergoes a gradual transition from Sudanian to Sahelian vegetation, with grasses predominantly forming at the end of the dry season and regenerating only after the onset of the first rains.

Key words: Chari-Logone, Lake Chad, rainfall, vegetation, spatio-temporel, NDVI.

INTRODUCTION

The past few decades have been marked by a sharp increase in the concentration of greenhouse gases in the atmosphere (Meyer, 1981). These aspects of recent environmental change are believed to be responsible for global (Houghton, 1992) and regional (Nicholson, 2001) climate change.

The Lake Chad basin and the Central Sahel, suffer from repeated droughts linked to rainfall variability and leading to uncertainties over surface water bodies and groundwater resources. Drought management practices require accurate estimates of rainfall in space and time (Joyce and Arkin, 1997; Verdin et al., 2016). Precipitation assessment is important for effective natural resource management and natural hazard mitigation (Leroux, 1986; Funk et al., 2015).

This concept of precipitation assessment is important in developing regions and areas prone to extreme events (Chevallier and Pouyaud, 1996). Meteorological data are used to provide early warning of extreme events (Verdin et al., 2016). However, actual observed data from meteorological stations are often limited in African regions, clustered in major cities (Rozante et al., 2010).

In the Lake Chad basin, meteorological data from the 1940 to 1960s have been collected by ORSTOM

*Corresponding author. E-mail: mnourabdallah@gmail.com.

researchers. However, these data are not sufficiently representative of more recent decades, particularly the new period from 1980 to 2010 (Delclaux et al., 2011; Descroix et al., 2013; Nour et al., 2021). Presently, the dataset provided by the National Meteorological Agency of Chad (ANAM) is limited in quantity compared to the expansive area that needs coverage for a comprehensive forecast of rainfall variability. The sparse distribution of weather stations within the basin, including Sarh, Moundou, Bongor, N'Djaména, Pala, Abéché, Amtiman, and Bousso, poses a challenge in achieving a detailed understanding of the spatio-temporal structure of rainfall and impedes the development of accurate forecasting models. While satellite-derived rainfall data, as suggested by Huffman et al. (1995), presents an intriguing alternative, it comes with potential limitations such as a tendency to underestimate rainfall event magnitudes due to reliance on satellite algorithms and the indirect correlation between satellite infrared observations and rainfall intensities (Xie and Arkin, 1997). In light of these challenges, it is imperative to establish specific methods dedicated to updating and supporting the study of the spatio-temporal distribution of rainfall in the Lake Chad basin. Such methodologies will prove essential as input parameters for hydrological models, recognizing rainfall as a fundamental factor in watershed studies.

Moreover, the spatio-temporal evolution of the vegetation is important in the estimation of the elements of the hydrological and climatic balance. It participates strongly in the evapotranspiration process. Spatial and temporal data on vegetation allow the assessment of deforestation, monitoring of bushfires, etc. (Jepsen et al., 2009). Studies around the world have shown that the state of land cover and land use are closely related to the amount of precipitation and surface water (Cornet and Rambal, 1981; Pierre et al., 2011). Work by Cissé (2016) and Herrmann and Stichler (1980) has highlighted that the relationship between vegetation change and rainfall could provide information to analyze environmental change in the Sahel.

Monitoring data on vegetation in the Lake Chad basin are scarce (Gbetkom et al., 2022). In the absence of monitoring data measured on the ground, satellite images permanently record vegetation cover and allow complex analyses of its spatial and temporal evolution (Gbetkom et al., 2022). Today there are several sensors (Spot, Landsat, Modis, etc.) that observe the globe continuously and provide good quality images. The principle of the sensors is based on the acquisition of signals of radiation or reflection of the object.

However, the evolution of vegetation cover in response to rainfall variations in the Chari-Logone watershed has not been studied. However, it is noted that a good knowledge of vegetation cover in response to rainfall may be necessary for good rainfall anticipation for agricultural planning and land use management. The objective of this study is to characterize the evolution of vegetation cover in response to rainfall in the Chari-Logone basin.

Description of the physical setting

Study area and geological setting

The Chari and Logone basin is the southern part of the Lake Chad basin between 6° and 14° North latitude and 12° and 24° East longitude. It covers an area of 612,933 km², and its shores are surrounded by a series of mountainous massifs: the Guera and Ouaddaï massifs, and the Kagas and Adamaoua ranges (Figure 1). The major geological features of the Chari and Logone basin have been extensively studied by Louis (1970). Two major geological units can be distinguished: (1) in the south and north-northeast, the Precambrian basement formations outcrop. This basement is essentially made up of granites, migmatites, gneisses, quartzites, amphibolites, schists and micaschists. The Logone basin drains granitic and magmatic terrains and the Chari basin drains gneisses, quartzites, amphibolites, schists and micaschists (Roche, 1980). (2) In the center and northwest, there is a series of sandstone sediment covers of Cenozoic age (terminal continental) and fluvial or fluvial-lacustrine formations of recent Quaternary age. The formation of the terminal continental consists essentially of clays and sands, which were emplaced during the period of successive transgressions and regressions of the mega-lake Chad (Pias, 1970).

Most of the soils in the Chari-Logone basin were formed on the fluvio-lacustrine alluvium of the Chadian basin (Boulvert, 1968; Pias, 1968). These are ferralitic sesquioxid soils that originate from granitic arenas.

Climate framework

The meteorological data described were collected from the Agence Nationale de Météorologie du Tchad (ANAM). The Chari-Logone basin has a contrasting tropical to Sahelian climate. The parameters studied here are temperature, rainfall, humidity, and evaporation for the period 1984-2014 at the N'Djamena and Sarh stations (Figure 1).

Temperature

Monthly temperature trends show two maxima: a peak in April, before the start of the rainy season, and a second peak in October, at the end of the rainy season (Figure 2). Interannual mean temperatures are highly variable (Nour et al., 2021).

Precipitation

Rainfall data from the two stations located in the Chari-Logone basin indicate that rainfall decreases from south to north. The southern station (Sarh) receives the most

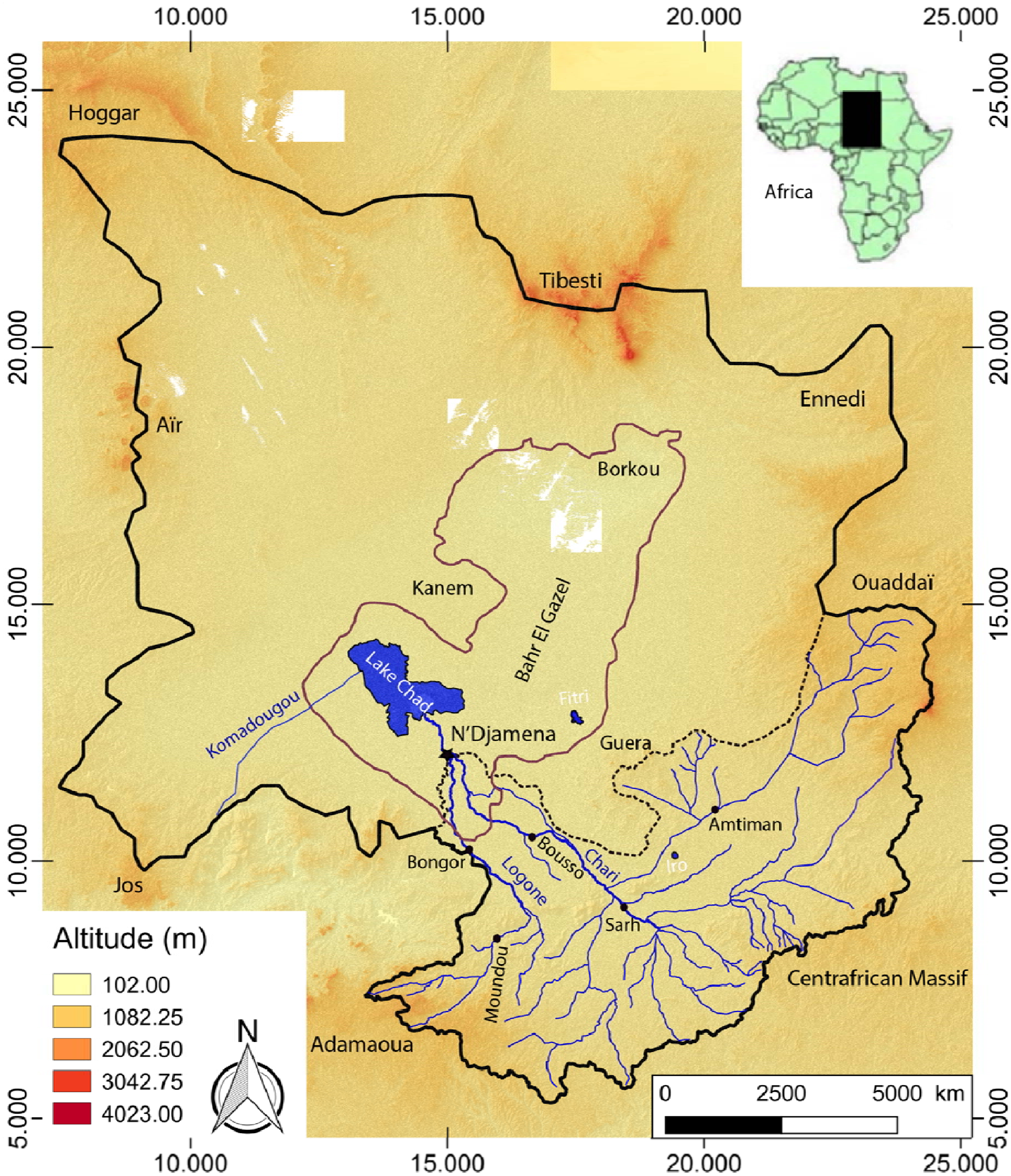

Figure 1. Map of the Lake Chad Basin. The black dotted line represents the boundary of the Chari-Logone basin and the brown line represents the surface of the lake reached during the mid-Holocene.

rainfall, with an annual average of 972 mm, while N'Djamena receives an average of 544 mm per year. In the southern part of the basin, the rainy season starts earlier than in the north (April), and ends later (October). Monthly trends show alternating wet and dry periods. This pattern of rainfall over the year shows that the Chari-Logone basin has a tropical rainfall regime with two seasons (Figure 3): a wet season (April to October) and a dry season (November to March). The length of the rainy season is not the same everywhere.

Atmospheric humidity

Air humidity follows the same seasonal pattern as rainfall (Figure 4). Air humidity varies according to wind

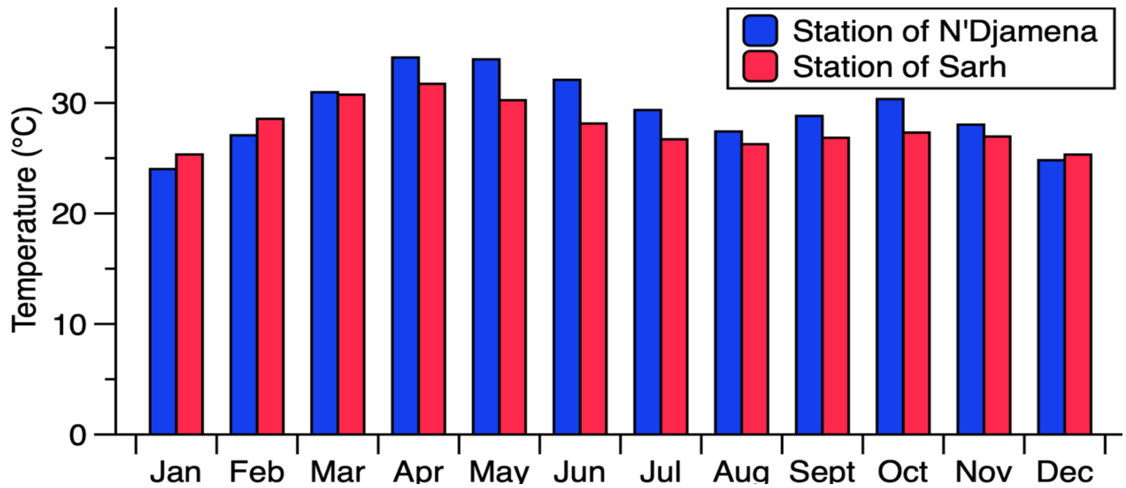

Figure 2. Temperature in N'Djamena and Sarh between 1984 and 2014.

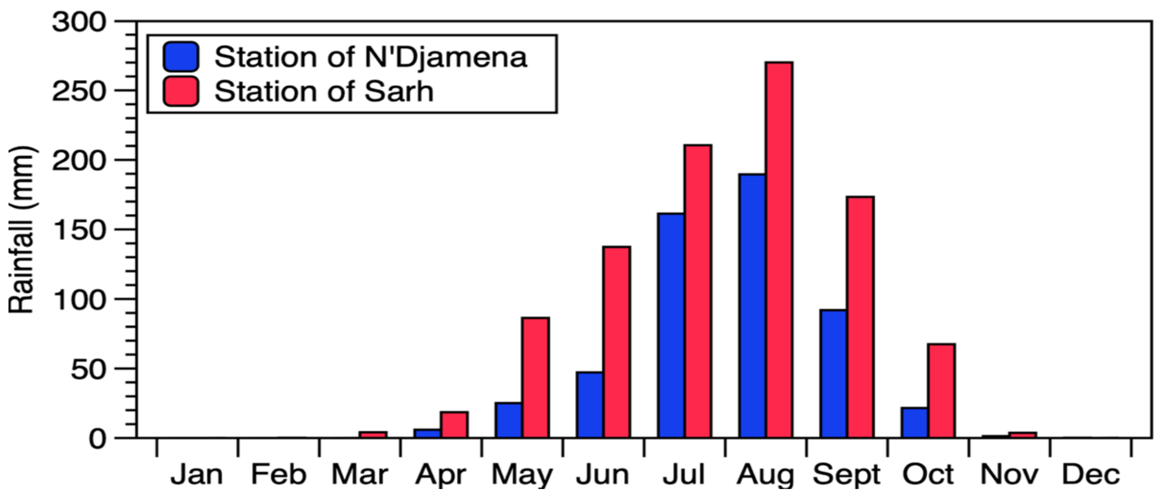

Figure 3. Rainfall in N'Djamena and Sarh from 1984 to 2014.

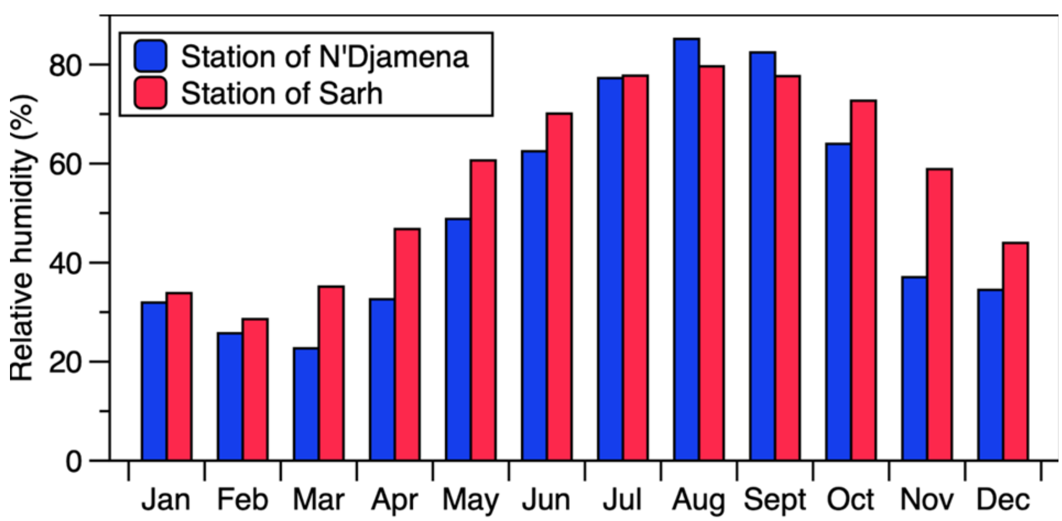

Figure 4. Relative humidity in N'Djamena and Sarh between 1984 and 2014.

frequency in the area.

Evaporation

Evaporation evolves in the same way as air temperature (Figure 6). The average monthly evaporation maximum is observed in March, reaching 281 and 416 mm in Sarh and N'Djamena, respectively.

Hydrological setting

The Chari-Logone basin is drained by two main river systems, the Logone and Chari. The Logone River, 1000 km long with an area of 90,000 km^2, has its source in the Adamawa plateau in Cameroon, with an altitude varying from 305 to 835 m (Cabot, 1965; Gac, 1980). The Chari is 1200 km long. The Chari basin covers an area of approximately $523,10^3$ km^2. The Chari originates in the Central African Republic at an altitude of 500 to 600 m. The Chari and Logone rivers meet at N'Djamena, 110 km upstream of Lake Chad (Figure 1). The base flow of the Chari-Logone is provided by only 12% of the catchment area (Bouchez et al., 2019).

METHODOLOGY

Rainfall data acquisition

Rainfall data for the Chari-Logone basin are derived from several sources such as: (1) a monograph of the Chari (Billon et al., 1974) using data from 74 stations throughout the watershed, covering periods of 6 to 34 years over a selected period from 1940 to 1967; (2) a monograph on the Logone (Cabot 1965) using data from about 30 stations on the Logone, with durations of 4 to 27 years; and (3) data from the National Meteorological Agency (ANAM): data from 8 stations from 1984 to 2014.

The rainfall is marked by a strong irregularity in its spatial and temporal distribution. Due to its high spatial heterogeneity, precipitation is a difficult parameter to quantify accurately. The ANAM data are the most recent, from 8 stations spread over the Chari-Logone basin (Mahamat Nour et al., 2021) and cover the period from 1984 to 2014.

Spatial interpolation using the Kriging method on very few stations (ANAM data) is not accurate. Data from the Logone (Cabot, 1965) and Chari (Billon et al., 1968) monographs were chosen for this section, because the stations, which are more numerous and closer together, are therefore more representative of rainfall in the Chari-Logone basin (Mahamat Nour, 2019), which made it possible to do a fairly accurate Kriging.

In the data processing phase, we followed a two-step approach: (1) identified common stations that span both the periods covered in the monographs and the period from 1984 to 2014 (ANAM). This analysis revealed 8 stations common to both datasets, as outlined in the work by Nour (2019). (2) Subsequently, the data from the two monographs was updated by applying a correction factor. This factor was calculated as the average ratio of the monograph data to the ANAM data, under the assumption that all rainfall stations in and around the basin exhibit similar evolution patterns with a shared influencing factor. This corrective process was systematically applied to all stations and for every month of the year. Further details on this methodology can be found in the work by Nour (2019). The selected Kriging method is employed in this study to characterize the distribution and variability of rainfall fields by interpolating and quantifying the estimation error of area averages. This method offers the dual advantage of providing the best linear unbiased estimate of rainfall at any given point and assessing the associated uncertainty linked to the estimate. The study focuses on seventy-one rainfall stations using monograph data, showcasing a relatively even distribution throughout the basin. The analyzed period spans from 1984 to 2014, and the dataset is reconstructed based on known data from 1927 to 1970.

Acquisition of vegetation data

The vegetation data in this study were derived from images captured by the Moderate Resolution Imaging Spectroradiometer (MODIS) sensor on board the TERRA satellite, providing a spatial resolution of 1000 m. MODIS operates on both the Terra and Aqua spacecraft, observing the entire Earth's surface every one to two days. The sensor utilizes detectors to measure 36 spectral bands spanning from 0.405 to 14.385 μm and acquires data at three spatial resolutions: 250, 500 and 1000 m. In recent years, the deployment of increasingly advanced sensors in orbit has enhanced and popularized the analysis of vegetation cover using biological indices. MODIS vegetation indices generated at regular intervals of a few days and at multiple spatial resolutions, contribute to the comprehensive assessment of vegetation dynamics. The index employed in this study is the normalized difference of spectral reflectance measurements obtained in the Near Infrared (NIR) and Red wavelength regions. Initially defined by Tucker (1979), this index is widely utilized in vegetation monitoring studies. It demonstrates stability that enables comparisons of vegetation activity at seasonal time intervals (Huete et al., 2002). NDVI is universally acknowledged by the scientific community for its reliability and direct correlation with canopy chlorophyll activity, facilitating the quantification of plant biomass production (Huete et al., 1997).

The equation for calculating NDVI is given by Tucker (1979) and can be written as follows:

$$NDVI = \frac{PIR - Red}{PIR + Red}$$

The NDVI value is a ratio calculated from two spectral bands: the red band, ranging from 0.73 to 1.1 μm, and the near-infrared band, ranging from 0.55 to 0.68 μm. Vegetation absorbs solar radiation in the red band and reflects it maximally in the near-infrared band. Clouds and water exhibit higher reflectance in the visible spectrum than in the infrared, resulting in negative NDVI values. Conversely, bare soil has comparable reflectance in both the visible and infrared, but its very low NDVI values, on either side of zero, prevent confusion with vegetation (Huete et al., 1997). The theoretical range of NDVI values is between -1 and 1. In practice, an open water surface typically has NDVI values close to 0, bare soil registers values between 0.1 and 0.2, while dense vegetation demonstrates values ranging from 0.5 to 0.8. MODIS data can be accessed on the NASA MODIS Data website: https://modis.gsfc.nasa.gov/data/, under the Vegetation Index (NDVI and EVI) tab. Consequently, we successfully accessed the archive of "Vegetation Indices Monthly L3 Global 1 km from TERRA PROD, MOD13A3," retrieving all raw images that encompass the Chari-Logone area from January 2013 to December 2015 at monthly intervals. To encompass the entirety of the Chari-Logone area, four bands of MODIS images are required to form a scene. Thus, the total number of bands for each month is 4 bands/month × 12 months × 3 years = 192 bands, corresponding to 36 scenes for the period spanning from 2013 to 2015. The processing of these

NDVI data followed several steps in different software (Envi, Qgis, Excel).

RESULTS AND DISCUSSION

Spatial and temporal evolution of precipitation

The spatial distribution of monthly rainfall, illustrated in Figure 5a to g, generally exhibits a decreasing gradient from south to north between April and October. The onset of the rainy season varies, initiating in April in the extreme south (Figure 5a), May in the central south, and June in the north of the basin (N'Djamena). During these months, the southern part experiences substantial rainfall amounts, ranging between 130 and 50 mm, while the northern part records minimal precipitation, barely exceeding 10 mm. The spatial evolution becomes irregular (Figure 5d and e) in July and August, the wettest periods, where orographic effects from mountain massifs (Guera) and the density of vegetation in the region (Salamat) likely exert a positive influence on rainfall phenomena. As the rainy season concludes in September (Figure 5d) and October (Figure 5d), the gradient reverses, witnessing a decrease in rainfall from north to south, aligning with the southward movement of the Inter-Tropical Convergence Zone (ITCZ) associated with the onset of the Harmattan. This reversal is attributed to the Adamaoua and Yadé massifs disrupting the monsoon's advance towards Chad (Cabot, 1965). Consequently, to the north of the Adamaoua massifs, the latitudinal zonation resumes, marked by a rapid decrease in rainfall.

Consistently, the highest rainfall values are recorded at the southwestern extremities, aligning with the entry path of the monsoon flow. This pattern corresponds to a gradual transition from the wetter Sudanian regions in the southwest (receiving between 1,300 and 800 mm) to the drier Sahelian regions in the northeast (with rainfall amounts ranging from 800 to 200 mm). The observed spatial distribution can be elucidated by the latitudinal or continental effect, attributed to the reduction in water content of the air mass carrying precipitation as it progresses inland. Notably, for the same latitude, mountainous regions receive a greater volume of precipitation compared to plains. The Chari-Logone basin is characterized by a tropical climate situated within the transitional zone of the intertropical front (ITF). This zone represents the convergence of two distinct air masses: the monsoon, which is humid and originates from the southwest, influenced by oceanic conditions, and the Harmattan, which is dry, emanates from the northeastern sector, and has a continental origin. The meeting point of these two air masses induces convergence in the deviated trade winds, leading to cloud formation and subsequent precipitation (Massuel, 2001). In comparison to the northern region, the rainy season in the Chari-Logone basin commences earlier (April) and concludes later (October), with an approximately one-month disparity (Figure 6). The data illustrates a progressive increase in rainfall, peaking in August before experiencing a sharp decline. The monthly pattern demonstrates a cyclical alternation between wet and dry periods. This temporal evolution highlights a tropical rainfall regime in the Chari-Logone basin, characterized by two seasons: a wet season from April to October and a dry season from November to March. Interestingly, unlike the rest of the year, the spatial distribution of rainfall levels does not adhere to a latitudinal gradient.

The climate in the Chari-Logone basin is influenced by the seasonal movement of two air masses separated by a front, as described by Olivry (2002). These air masses consist of the humid monsoon originating from the southwest sector with oceanic influence and the dry Harmattan originating from the northeastern sector with continental origin (Nicholson, 2015; Lienou, 2007; Leroux, 1986). The seasonal shift in the Intertropical Discontinuity (ITD) contributes to variability in rainfall patterns within the Chari-Logone basin. A gradual northward movement of the Intertropical Convergence Zone (ITCZ) results in rainfall in the southern part of the Chari-Logone basin. Subsequently, the ITCZ reaches its northernmost position in July-August, marking the wettest months of the year. In September-October, the ITCZ undergoes a rapid southward movement (Nicholson, 2000). The dry season initiates in early October in the northern part of the country, while in the south, rains may persist until November.

Spatial and temporal distribution of vegetation covers during the annual cycle

The diagram in Figure 8 illustrates that rainfall initiates in April, peaks in August, and concludes in October, with minimal interannual variability. However, the year 2014 appears to be wetter than both 2013 and 2015. The NDVI value exhibits a progressive increase with the onset of rainfall, reaching its zenith in July for the Moundou basin and in August for the Sarh and N'Djamena basins (Figures 7 and 8). Subsequently, it gradually decreases, reaching a minimum observed in February. The temporal evolution of NDVI over the three years of observation does not demonstrate significant annual variability.

Figure 9 provides a comprehensive depiction of both spatial and seasonal changes. The observed seasonal evolution of vegetation in the Chari-Logone basin aligns with that of climate, particularly rainfall (Figure 8). Previous studies (Pias, 1968; Maley and Maley, 1981) and recent investigations have consistently shown that vegetation in the basin undergoes a gradual transition from Sudanian to Sahelian vegetation. The Sudanian vegetation consists of wooded savannah with forest galleries and the Sahelian vegetation is composed of two elements:

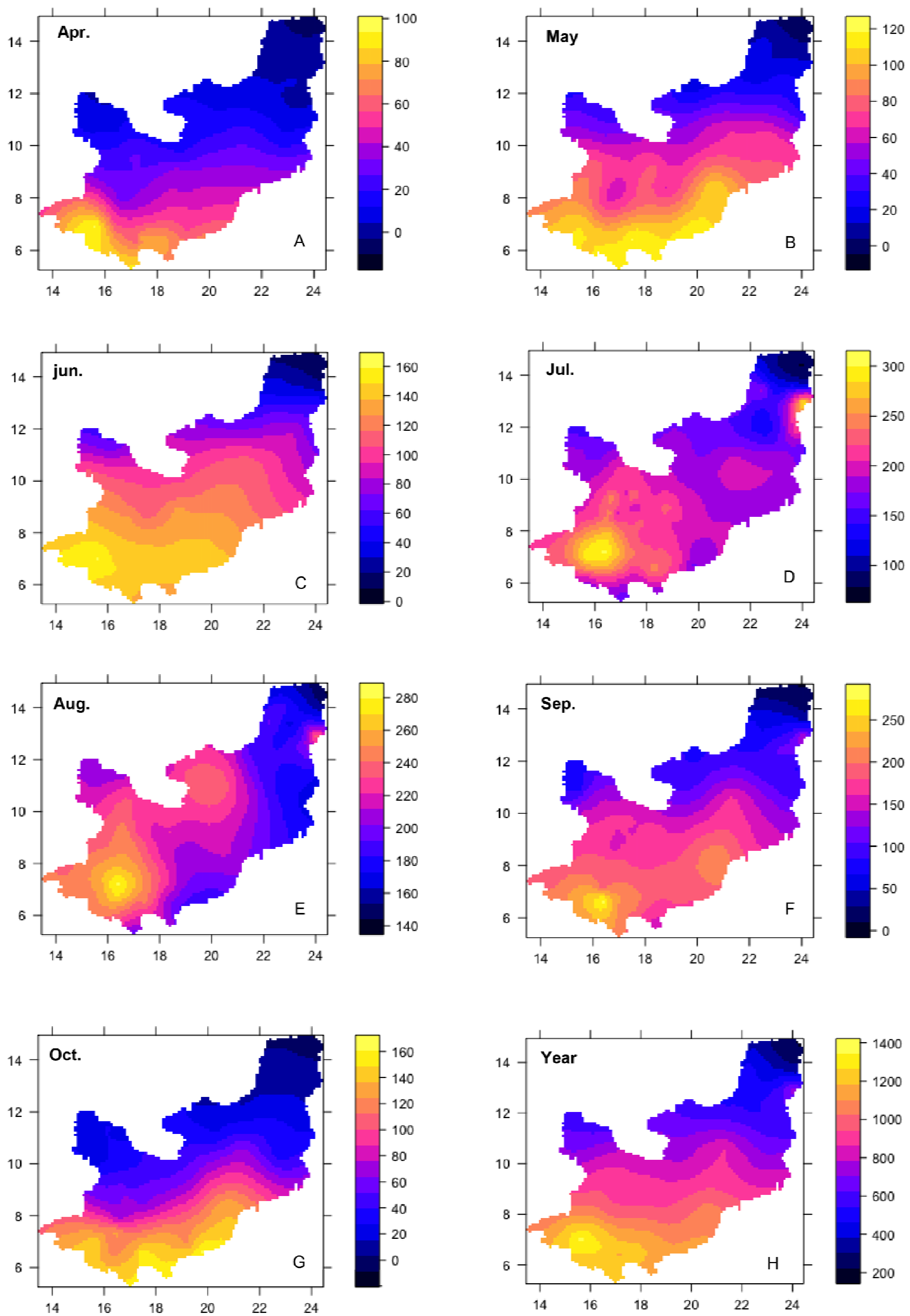

Figure 5. Spatio-temporal distribution of rainfall in the Chari-Logone basin.

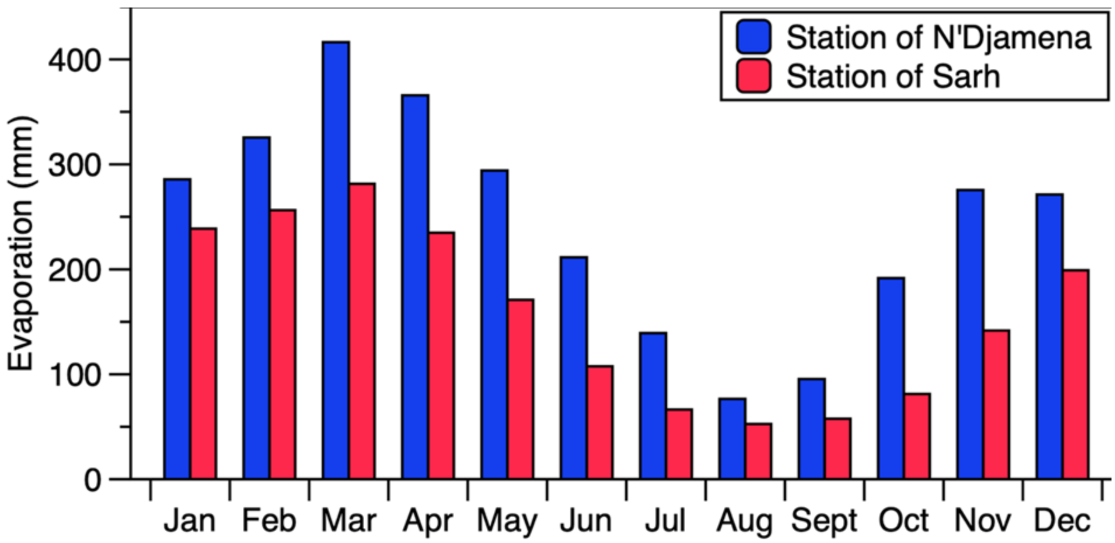

Figure 6. Monthly evaporation (Piche technique) in N'Djamena and Sarh between 1984 and 2014.

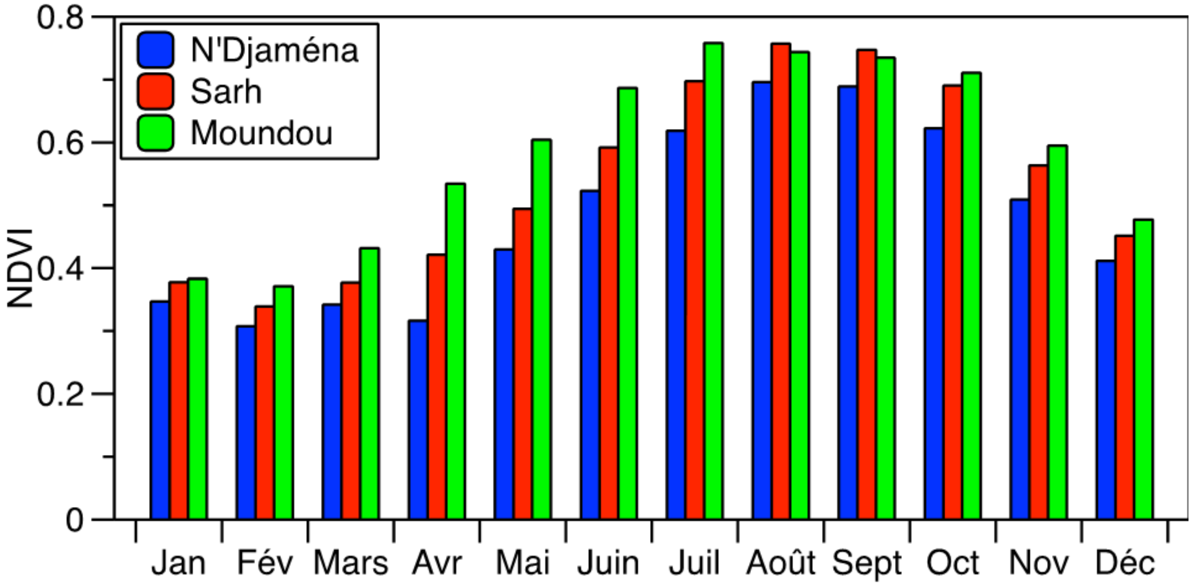

Figure 7. Seasonal evolution of normalized difference of spectral reflectance measurements acquired in the 'Near Infra-Red' (PIR) and 'Red' (NDVI) wavelength zones (Chari-Logone sub-basins) for the year 2015.
Source: Data modis web naza.

1) A herbaceous stratum, essentially composed of annual plants dominated by grasses
2) A stand of woody plants (trees and shrubs) dominated mainly by thorny plants.

Vegetation undergoes various transformations under the action of man and the influence of climatic hazards. Under a hot and dry climate, marked by large interannual variations in rainfall, all plant formations are open, discontinuous in time and space. The herbaceous cover, formed mostly of grasses, largely disappears at the end of the dry season only to regenerate after the first rainfall (Roche, 1980).

The vegetation cover in the study area can have a strong influence on infiltration and evaporation, even at great depths, and knowledge of the plant formations in our area can support hypotheses of high evapotranspiration (Djoret and Favreau, 2014). Overall, from south to north, open forest and wooded shrub savanna evolve into Acacia shrub and herb steppe.

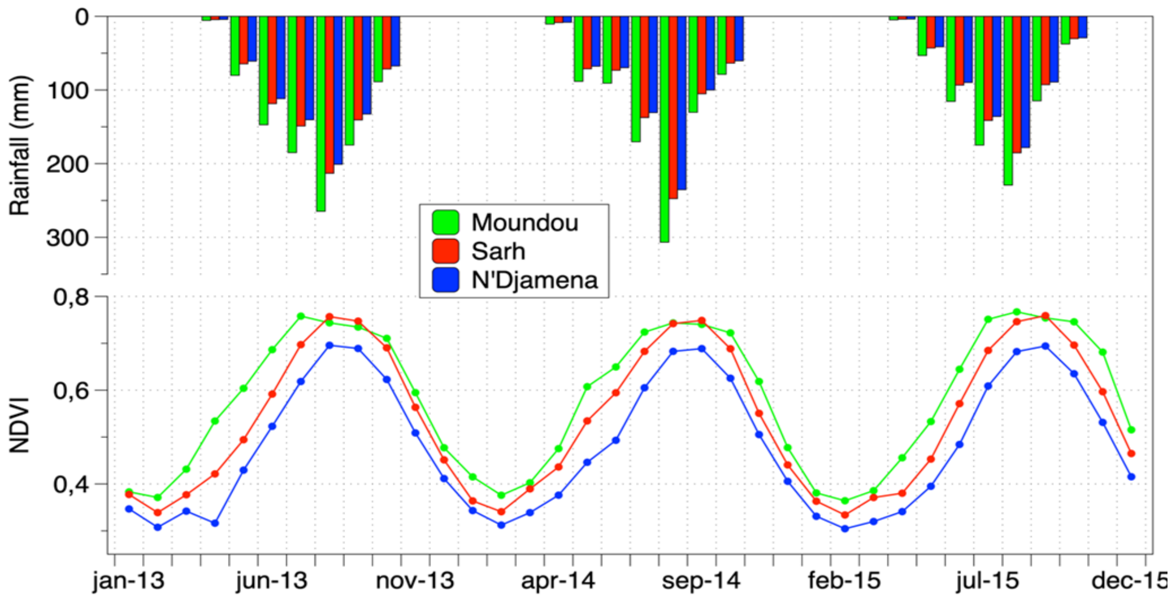

Figure 8. Evolution of precipitation and vegetation in the sub-basins of the Chari-Logone for the hydrological cycles from 2013 to 2015.

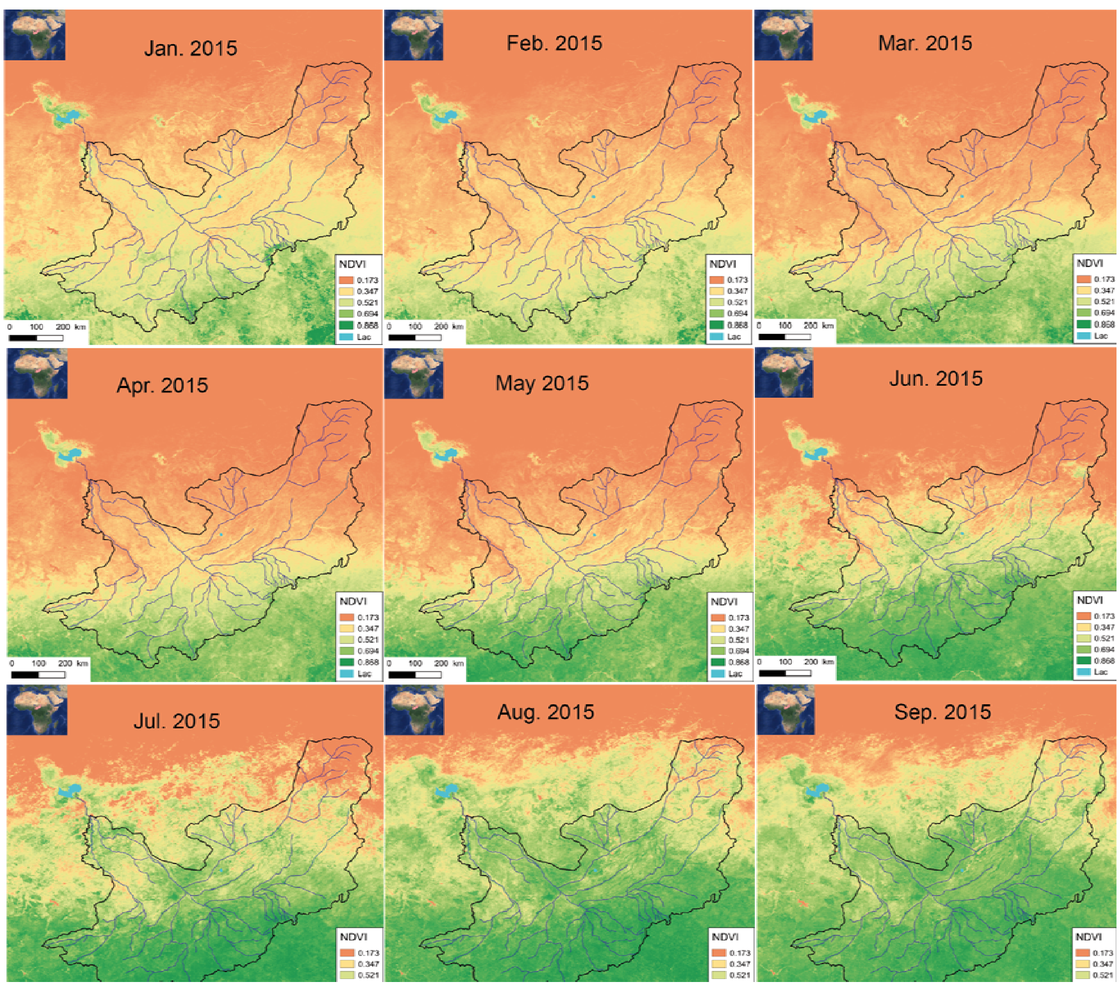

Figure 9. Spatial and temporal evolution map of the vegetation in the Chari - Logone basin for the year 2015.

Conclusion

The Chari-Logone basin exhibits a tropical climate, and the annual precipitation distribution predominantly follows a south-north gradient. The highest precipitation values are consistently recorded at the southwestern extremities, aligning with the entry path of the monsoon flow. This gradient signifies a gradual transition from the wetter Sudanian regions in the southwest (with precipitation ranging from 1,300 to 800 mm) to the drier Sahelian regions in the northeast (receiving between 800 and 200 mm). The onset of the rainy season precedes that in the south, commencing in April and concluding later in October. The seasonal shift in the Intertropical Discontinuity (ITD) contributes to the observed variability in the rainfall regime of the Chari-Logone basin. The basin experiences two distinct seasons: a short rainy season centered on summer (June-September) and a long dry season centered on winter. The NDVI value exhibits a progressive increase from March, reaching its peak in July or August in the southern part of the basin. Subsequently, it gradually decreases, with the lowest values observed in February. The seasonal evolution of vegetation in the Chari-Logone basin closely mirrors that of the climate, particularly rainfall, as the vegetation undergoes a gradual transition from Sudanian to Sahelian characteristics.

CONFLICT OF INTERESTS

The authors have not declared any conflict of interests.

REFERENCES

Billon B, Guiscafré J, Herbaud J, Oberlin G (1968). Monographie hydrologique du Chari. ORSTOM, Paris.

Bouchez C, Deschamps P, Goncalves J, Hamelin B, Mahamat Nour A, Vallet-Coulomb C, Sylvestre F (2019). Water transit time and active recharge in the Sahel inferred by bomb-produced 36Cl. Scientific Reports 9:7465. https://doi.org/10.1038/s41598-019-43514-x

Cabot J (1965). Le bassin du moyen Logone, Mémoires ORSTOM. ORSTOM, Paris.

Chevallier P, Pouyaud B (1996). La distribution spatio-temporelle des pluies au Sahel: Apport de l'experience EPSAT Niger. IAHS.

Cissé S (2016). Étude de la variabilité intra saisonnière des précipitations au Sahel: impacts sur la végétation (cas du Ferlo au Sénégal) (PhD Thesis). Université Pierre et Marie Curie-Paris VI; Université Cheikh Anta Diop (Dakar).

Cornet A, Rambal S (1981). Simulation de l'utilisation de l'eau par une phytocenose de la zone sahélienne au Sénégal test de deux modèles, in: Proceedings of the 9th Symposium Informatique et Biosphère on "hydrologie, Cycle de l'eau et Informatique pp. 156-179.

Delclaux F, Seignobos C, Liénou G, Genthon P (2011). Water and people in the Yaere floodplain (NorthCameroon). In Foodplains. ed. Marc A. Alvarez pp. 1-36.

Descroix L, Diongue Niang A, Dacosta H, Panthou G, Quantin G, Diedhiou A (2013). Évolution des pluies de cumul élevé et recrudescence des crues depuis 1951 dans le bassin du Niger moyen (Sahel). Climatologie pp. 37-49.

Djoret D, Favreau G (2014). Ressources en eau souterraine et relations avec le Lac.

Funk C, Verdin A, Michaelsen J, Peterson P, Pedreros D, Husak G (2015). A global satellite assisted precipitation climatology. https://doi.org/10.5194/essd-7-275-2015

Gac JY (1980). Géochimie du bassin du lac Tchad: Bilan de l'altération de l'érosion et de la sédimentation. ORSTOM, Paris.

Gbetkom PG, Crétaux JF, Tchilibou M, Carret A, Delhoume M, Bergé-Nguyen M, Sylvestre F (2022). Lake Chad vegetation cover and surface water variations in response to rainfall fluctuations under recent climate conditions (2000-2020). Science of The Total Environment 159302.

Herrmann A, Stichler W (1980). Groundwater-runoff relationships. CATENA 7:251–263. https://doi.org/10.1016/0341-8162(80)90011-9

Houghton JT (1992). Climate Change 1992.

Huete A, Didan K, Miura T, Rodriguez EP, Gao X, Ferreira LG (2002). Overview of the radiometric and biophysical performance of the MODIS vegetation indices. Remote sensing of environment 83:195-213.

Huete AR, Liu HQ, Batchily KV, Van Leeuwen W (1997). A comparison of vegetation indices over a global set of TM images for EOS-MODIS. Remote sensing of environment 59:440-451.

Huffman GJ, Adler RF, Rudolf B, Schneider U, Keehn PR (1995). Global Precipitation Estimates Based on a Technique for Combining Satellite-Based Estimates, Rain Gauge Analysis, and NWP Model Precipitation Information. Journal of Climate 8(5):1284-1295. https://doi.org/10.1175/1520-0442(1995)008<1284:GPEBOA>2.0.CO;2

Jepsen JU, Hagen SB, Høgda KA, Ims RA, Karlsen SR, Tømmervik H, Yoccoz NG (2009). Monitoring the spatio-temporal dynamics of geometrid moth outbreaks in birch forest using MODIS-NDVI data. Remote Sensing of Environment 113(9):1939-1947.

Joyce R, Arkin PA (1997). Improved Estimates of Tropical and Subtropical Precipitation Using the GOES Precipitation Index. J. Atmos. Oceanic Technol. 14:997-1011. https://doi.org/10.1175/1520-0426(1997)014<0997:IEOTAS>2.0.CO;2

Leroux M (1986). L'Anticyclone mobile Polaire : facteur premier de la climatologie tempérée (The Polar mobile Anticyclone : first factor of temperate climatology). Bulletin de l'Association de Géographes Français 63(4):311-328. https://doi.org/10.3406/bagf.1986.1354

Lienou G (2007). Impacts de la variabilité climatique sur les ressources en eau et les transports de matières en suspension de quelques bassins versants représentatifs au Cameroun. These de doctorat PhD, université de Yaoundé I.

Louis P (1970). Contribution géophysique à la connaissance géologique du bassin du lac Tchad, Mémoires ORSTOM. ORSTOM, Paris.

Mahamat Nour A (2019). Fonctionnement hydrologique, chimique et isotopique du principal affluent du lac Tchad: le système Chari-Logone (These de doctorat). Aix-Marseille.

Mahamat Nour A, Vallet-Coulomb C, Gonçalves J, Sylvestre F, Deschamps P (2021). Rainfall-discharge relationship and water balance over the past 60 years within the Chari-Logone sub-basins, Lake Chad basin. Journal of Hydrology: Regional Studies 35:100824. https://doi.org/10.1016/j.ejrh.2021.100824

Maley J (1981). Etudes palynologiques dans le bassin du Tchad et paléoclimatologie de l'Afrique nord-tropicale de 30 000 ans à l'époque actuelle.

Meyer LD (1981). How Rain Intensity Affects Interrill Erosion. Transactions of the ASAE 24(6):1472-1475. https://doi.org/10.13031/2013.34475

Massuel S (2001). Modélisation hydrodynamique de la nappe phréatique quaternaire du bassin du lac Tchad. DEA, Univ. Montpellier II/Univ. d'Avignon et des pays du Vaucluse 85.

Nicholson S (2000). Land surface processes and Sahel climate. Reviews of Geophysics 38(1):117-139. https://doi.org/10.1029/1999RG900014

Nicholson SE (2015). Evolution and current state of our understanding of the role played in the climate system by land surface processes in semi-arid regions. Global and Planetary Change 133:201-222. https://doi.org/10.1016/j.gloplacha.2015.08.010

Nicholson SE (2001). Climatic and environmental change in Africa during the last two centuries. Climate Research 17(2):123-144. https://doi.org/10.3354/cr017123

Olivry JC (2002). Synthèse des connaissances hydrologiques et potentiel en ressources en eau du fleuve Niger. World Bank, Niger

Basin Authority, provisional report 160.
Pias J (1970). La végétation du Tchad: ses rapports avec les sols, variations paléobotaniques au quaternaire; contribution à la connaissance du bassin tchadien. IRD Editions.
Pias J (1968). Contribution à l'étude des formations sédimentaires tertiaires et quaternaires de la cuvette tchadienne et des sols qui en dérivent (République du Tchad) (PhD Thesis). Orstom, Paris P 527.
Pierre C, Bergametti G, Marticorena B, Mougin E, Lebel T, Ali A (2011). Pluriannual comparisons of satellite-based rainfall products over the Sahelian belt for seasonal vegetation modeling. Journal of Geophysical Research: Atmospheres 116 p.
Roche MA (1980). Traçage naturel salin et isotopique des eaux du système hydrologique du lac Tchad. ORSTOM, Paris.
Rozante JR, Moreira DS, Goncalves LGG, Vila DA (2010). Combining TRMM and Surface Observations of Precipitation: Technique and Validation over South America. Wea. Forecasting 25(3):885-894. https://doi.org/10.1175/2010WAF2222325.1
Tucker CJ (1979). Red and photographic infrared linear combinations for monitoring vegetation. Remote sensing of Environment 8(2):127-150.
Verdin A, Funk C, Rajagopalan B, Kleiber W (2016). Kriging and Local Polynomial Methods for Blending Satellite-Derived and Gauge Precipitation Estimates to Support Hydrologic Early Warning Systems. IEEE Transactions on Geoscience and Remote Sensing 54(5):2552-2562. https://doi.org/10.1109/TGRS.2015.2502956
Xie P, Arkin PA (1997). Global Precipitation: A 17-Year Monthly Analysis Based on Gauge Observations, Satellite Estimates, and Numerical Model Outputs. Bull. Amer. Meteor. Soc. 78(11):2539-2558. https://doi.org/10.1175/1520-0477(1997)078<2539:GPAYMA>2.0.CO;2